AD-A182 930 ASSESSMENT OF EXCITATION MECHANISMS AND TEMPORAL DEPENDENCIES OF INFRARED..(U) UTAH STATE UNIV LOGAN CENTER FOR SPACE ENGINEERING C E KOLB ET AL. 31 MAR 87 CSE/87-016 AFGL-TR-87-0129 F19628-83-C-0056 F/G 4/1 1/1

UNCLASSIFIED NL

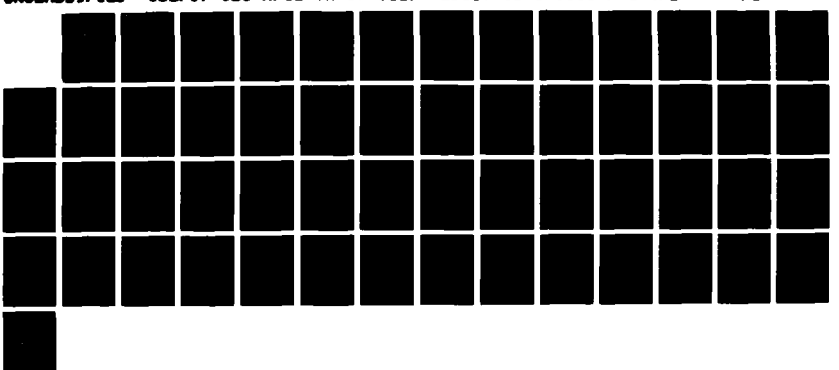

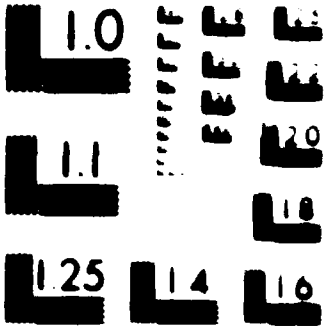
1.0
1.1
1.25
1.4
1.6

(12)

AFGL-TR-87-0129

ASSESSEMENT OF EXCITATION MECHANSIMS AND TEMPORAL DEPENDENCIES OF INFRARED RADIATION FROM VIBRATIONALLY EXCITED CARBON MONOXIDE AND OZONE IN EXCEDE EXPERIMENTS

By

C.E. Kolb, M.S. Zahniser, and R.B. Lyons

Center for Chemical and Environmental Physics
Aerodyne Research, Inc.
45 Manning Road
Billerica, MA 01821

The work reported herein was performed under subcontract to
Center for Space Engineering
Utah State University
Logan, UT 84322-4140

Scientific Report No. 22

31 March 1987

Prepared for:

AIR FORCE GEOPHYSICS LABORATORY
AIR FORCE SYSTEMS COMMAND
UNITED STATES AIR FORCE
HANSCOM AIR FORCE BASE, MA 01731

Unclassified
SECURITY CLASSIFICATION OF THIS PAGE

AD-A180 430

REPORT DOCUMENTATION PAGE

1a. REPORT SECURITY CLASSIFICATION: Unclassified	1b. RESTRICTIVE MARKINGS:
2a. SECURITY CLASSIFICATION AUTHORITY:	3. DISTRIBUTION/AVAILABILITY OF REPORT: Approved for public release; distribution unlimited.
2b. DECLASSIFICATION/DOWNGRADING SCHEDULE:	
4. PERFORMING ORGANIZATION REPORT NUMBER(S): CSE/87-016	5. MONITORING ORGANIZATION REPORT NUMBER(S): AFGL-TR-87-0129
6a. NAME OF PERFORMING ORGANIZATION: Center for Space Engineering; 6b. OFFICE SYMBOL (If applicable):	7a. NAME OF MONITORING ORGANIZATION: Air Force Geophysics Laboratory, Infrared Technology Division
6c. ADDRESS (City, State and ZIP Code): Utah State University, Logan, UT 84322-4140	7b. ADDRESS (City, State and ZIP Code): Hanscom Air Force Base, MA 01731
8a. NAME OF FUNDING/SPONSORING ORGANIZATION: Air Force Geophysics Lab, Infrared Technology Division; 8b. OFFICE SYMBOL (If applicable):	9. PROCUREMENT INSTRUMENT IDENTIFICATION NUMBER: F19628-83-C-0056
8c. ADDRESS (City, State and ZIP Code): Hanscom Air Force Base, MA 01731	10. SOURCE OF FUNDING NOS.

PROGRAM ELEMENT NO.	PROJECT NO.	TASK NO.	WORK UNIT NO.
62101F	7670	10	AK

11. TITLE (Include Security Classification): Assessment of Excitation Mechanisms (cont.)

12. PERSONAL AUTHOR(S): Charles E. Kolb, Mark S. Zahniser, Robert B. Lyons

13a. TYPE OF REPORT	13b. TIME COVERED	14. DATE OF REPORT (Yr., Mo., Day)	15. PAGE COUNT
Scientific No. 22	FROM 1/83 TO 11/84	1987 March 31	54

16. SUPPLEMENTARY NOTATION:

17. COSATI CODES			18. SUBJECT TERMS (Continue on reverse if necessary and identify by block number)
FIELD	GROUP	SUB. GR.	EXCEDE, artificial aurora, electron beam, CO, O_3, vibrational excitation mechanism, mechanism, chemiluminescence

19. ABSTRACT (Continue on reverse if necessary and identify by block number)

A goal of the EXCEDE artificial aurora experiment is to quantify upper atmospheric infared emission mechanisms for disturbed atmospheric conditions.

In this report sources and vibrational excitation mechanisms relevant to electron beam induced infrared emission from carbon monoxide and ozone in the 90-130 km altitude range are reviewed and assessed. Estimates of vibrational excitation deposition fractions ratioed to the ion pair creation energy deposition level are presented along with predicted energy deposition and decay rates for each mechanism. Mechanisms considered for CO(v) production include direct electron impact on ambient CO, dissociative excitation of CO_2, V-V exchange with vibrationally excited N_2, O_2 and O, and infrared chemiluminescence from the reaction of CO_2 with O^+. The conclusions are that the initial production of CO(v) (cont.)

20. DISTRIBUTION/AVAILABILITY OF ABSTRACT	21. ABSTRACT SECURITY CLASSIFICATION
UNCLASSIFIED/UNLIMITED ☒ SAME AS RPT. ☐ DTIC USERS ☐	Unclassified

22a. NAME OF RESPONSIBLE INDIVIDUAL	22b. TELEPHONE NUMBER (Include Area Code)	22c. OFFICE SYMBOL
Francis X. Robert	617 377-3614	AFGL/LSP

DD FORM 1473, 83 APR — EDITION OF 1 JAN 73 IS OBSOLETE.

Unclassified
SECURITY CLASSIFICATION OF THIS PAGE

Continued Block 11: and Temporal Dependencies of Infrared Radiation from Vibrationally Excited Carbon Monoxide and Ozone in EXCEDE experiments

Continued Block 19: 000045

is dominated by direct electron impact on ambient CO which represents a fraction of 4.5×10^{-5} of the ion pair production energy at 100 km altitude and decays with a radiative time constant of 28.3 ms. On a longer time scale of 0.1 to 100 s after electron beam termination, energy transfer from $N_2(A)$ and the $O_2(A',c)$ metastable states and from vibrationally excited $N_2(v)$ may contribute to $CO(v)$ production.

Potentially the strongest production mechanisms for vibrationally excited O_3 are the two body reactions of $O_2(A,A',c)$ metastable states with ambient O_2. These would occur on a time scale of 5 to 50 s and could account for up to 1% of the beam energy. Direct excitation of ambient O_3 by electron impact or by $O_2(b\ ^1\Sigma)$ quenching may contribute to prompt emission of $O_3(\nu_3)$ 9.6 μm radiation below 100 km.

FOREWORD

EXCEDE is a Defense Nuclear Agency/Air Force Geophysics Laboratory (DNA/AFGL) program which promotes the study of atmospheric radiative processes resulting from the controlled deposition of energetic electrons. A major goal of the EXCEDE experimental series is to generate a quantitative understanding of electron impact-induced infrared processes. In the experiments, rocket-borne electron accelerators introduce artificial auroral conditions into the upper mesosphere and lower thermosphere. The accompanying payload instrumentation then gathers and records the ultraviolet, visible, and infrared atmospheric emission data.

EXCEDE:SPECTRAL, the most recent EXCEDE mission, flew on 19 October 1979 into a dark, clear and aurorally inactive night atmosphere from Poker Flat, Alaska. EXCEDE:SPECTRAL, in contrast to previous EXCEDE missions, provided a higher irradiation rate, and incorporated more payload instruments. The payload optical and infrared spectral instruments recorded detailed band profiles.

The Center for Space Engineering (CSE) at Utah State University awarded Subcontract No. 83-035 to Aerodyne Research, Incorporated authorizing them to analyze data from EXCEDE:SPECTRAL. More specifically, they analyzed the 4.7μm carbon monoxide emission and ozone emissions ranging from 9.1 to 14.1μm. Aerodyne scientists completed their work under the subcontract and submitted their final report to CSE in December, 1984. This scientific report is based on Aerodyne's final report. It discusses direct excitation of CO and Aerodyne's temporal predictions for CO. This report also discusses the production mechanisms for vibrationally-excited ozone.

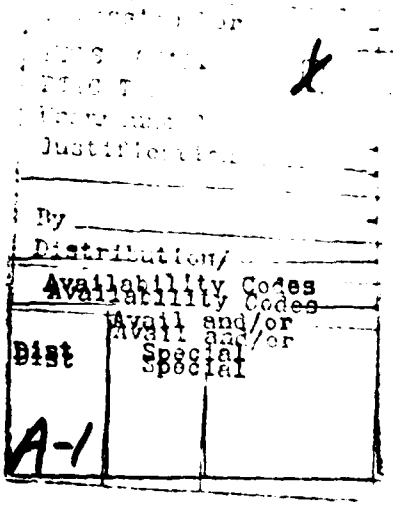

This page intentionally left blank.

TABLE OF CONTENTS

This page intentionally left blank.

LIST OF FIGURES

LIST OF TABLES

This page intentionally left blank.

1. INTRODUCTION

The EXCEDE series of experiments conducted for the Defense Nuclear Agency by the Air Force Geophysics Laboratory is designed to identify and quantify radiation producing mechanisms operative in the upper mesosphere and lower thermosphere during disturbances initiated by the deposition of high energy electrons.

During the EXCEDE experiments rocket borne electron accelerators deposit bursts of energetic (~ 3 kV) primary electrons at altitudes ranging from roughly 70 to 130 km. Ultraviolet, visible and infrared atmospheric emissions induced by these electron bursts are recorded by ground based, aircraft based and/or on-board (rocket based) spectrometers, radiometers and cameras.

A major goal of the EXCEDE experimental series is to generate a quantitative understanding of electron impact induced infrared processes. These processes, which, due to atmospheric transmission characteristics, must generally be observed by in situ instrumentation, were a major target of the EXCEDE:SPECTRAL mission flown in October, 1979.[1] While many of the infrared spectral features observed on this flight were anticipated, several infrared features observed by the EXCEDE:SPECTRAL flight were unexpected, including a distinct feature at 4.7 μm. In addition, the EXCEDE:SPECTRAL on-board instruments did not cover the spectral range between 6.8 and 12 μm.[1]

The field data gathered by the initial EXCEDE:SPECTRAL flight were rich in detail and subsequent analyses have highlighted the desirability of additional EXCEDE missions.[2] For instance, an analysis effort at Aerodyne Research, Inc. identified the source of the unexpected 4.7 μm feature as direct excitation of ambient thermospheric carbon monoxide.[3]

Furthermore, additional analyses of the long-lived visible spectral glow observed during the PRECEDE portion of the EXCEDE experimental series has

identified the 4.5-5.0 eV states (A $^3\Sigma^+$, A' $^3\Delta$ and c $^1\Sigma^-$) of O_2 as an important reservoir of electron deposition energy.[4,5] Quite recently, laboratory experiments involving these highly excited molecular oxygen states have strongly indicated that they can be a source of vibrationally excited ozone,[6] thus possibly producing strong infrared radiation in the 9.0 to 10.5 μm region not covered in the EXCEDE:SPECTRAL experiment.

The purpose of this report is to assess sources and vibrational excitation mechanisms for carbon monoxide and ozone in the disturbed atmosphere at altitudes (100-130 km) where the EXCEDE experimental arrangement functions best. Estimates of the source strength, spectral extent and temporal dependence of infrared radiation from vibrationally excited CO and O_3 induced by the EXCEDE electron impact source are presented along with suggestions on how future EXCEDE experiments might best be configured to observe the predicted infrared emission features.

2. INFRARED EMISSION FROM CARBON MONOXIDE

2.1 Direct Excitation of CO/Analysis of EXCEDE Spectral Observations

As reported in Reference 3, the 4.7μm emission feature measured by the EXCEDE:SPECTRAL experiment has been identified as arising from electron impact excited carbon monoxide. This identification was based on the shape of the spectral profile as measured by the on-board CVF spectrometer and on the close match between the magnitude of the observed radiance in the 4.7μm feature and that calculated using a thermospheric CO abundance predicted by Allen et al,[7] known direct electron impact cross sections for CO[8], and an energy deposition computer model devised by J. Winnick of AFGL.

The predicted carbon monoxide mixing ratio used in the model calculation is based on a photochemical model driven by the photodissociation of CO_2 above 90 km and the reaction of CO with OH to reform CO_2 below 90 km.[7] The resulting calculated CO and CO_2 profiles from Reference 7 are shown in Figure 2-1 along with a comparison to available CO measurements in the 50 to 80 km range[7,9,10] and measured CO_2 profiles in the 80 to 120 km range.[11] The good agreement in the CO_2 mixing ratio fall off above 90 km gives added weight to the predicted CO profile in the 90 to 120 km range.

The resulting CO and CO_2 profiles of Allen et al are also plotted in Figure 2-2 along with the other atmospheric constituents considered in the report. Major species profiles are adopted from the model of Keneshea et al.[12] The apparent variability in atomic oxygen in this altitude region is illustrated with data from several recent measurements.[13-15] The Ar, O_3 and NO profiles are taken from References 16-18.

The direct excitation of carbon monoxide vibrational states by secondary electrons occurs principally through a negative ion shape resonance in the 1 to 3 eV energy range.[19] The peak excitation energies for the first four vibrational levels lie just below the energy range for the 2 to 4 eV shape

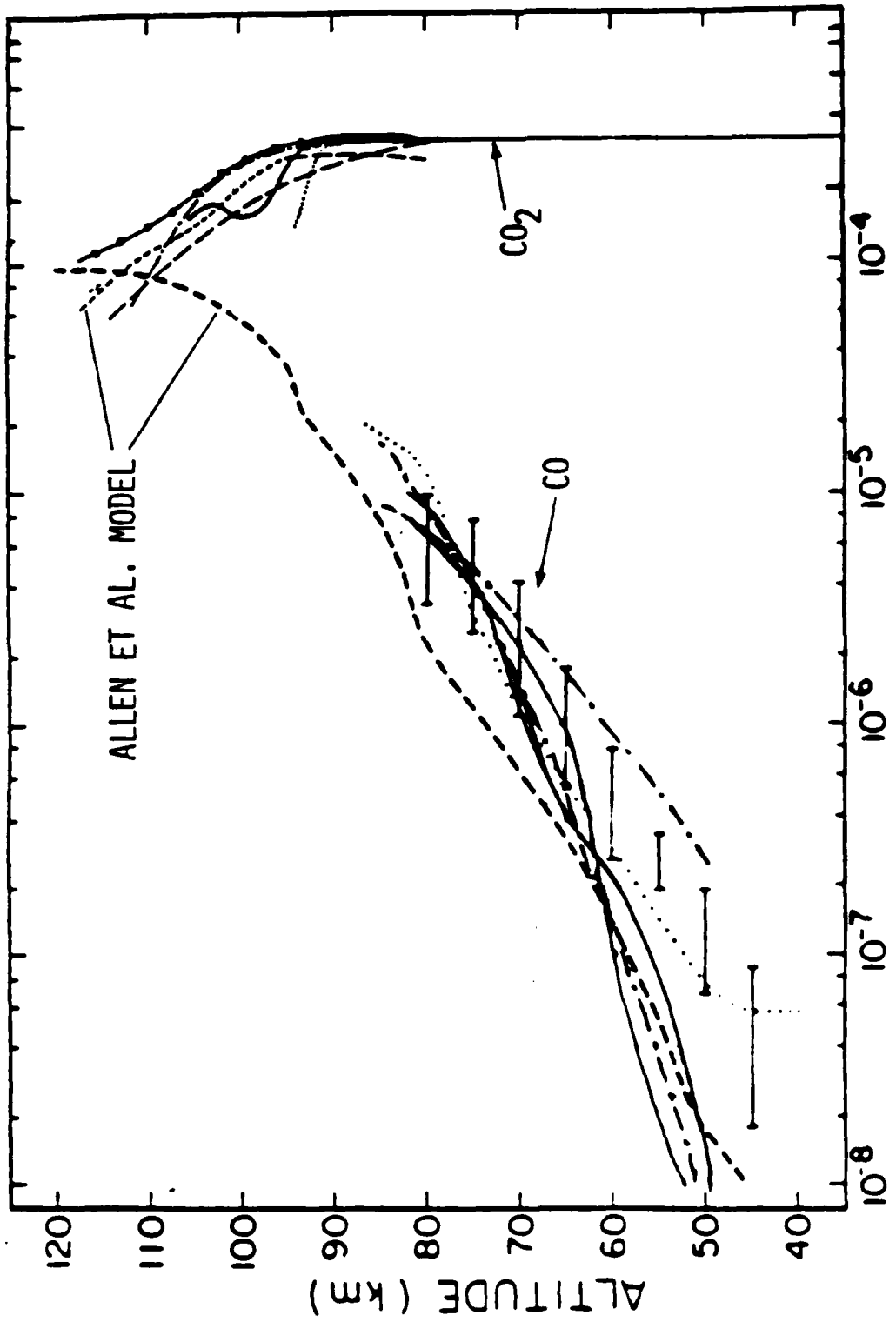

Figure 2-1. CO and CO_2 Mixing Ratios, Comparison of Model and Measurements. (Heavy and light dashed lines are model CO and CO_2 profiles respectively for CO, ... and ⊢⊣ data profiles are reproduced from Ref. 7, — · — from Ref. 9 and —— from Ref. 10, CO_2 profiles are from Ref. 11)

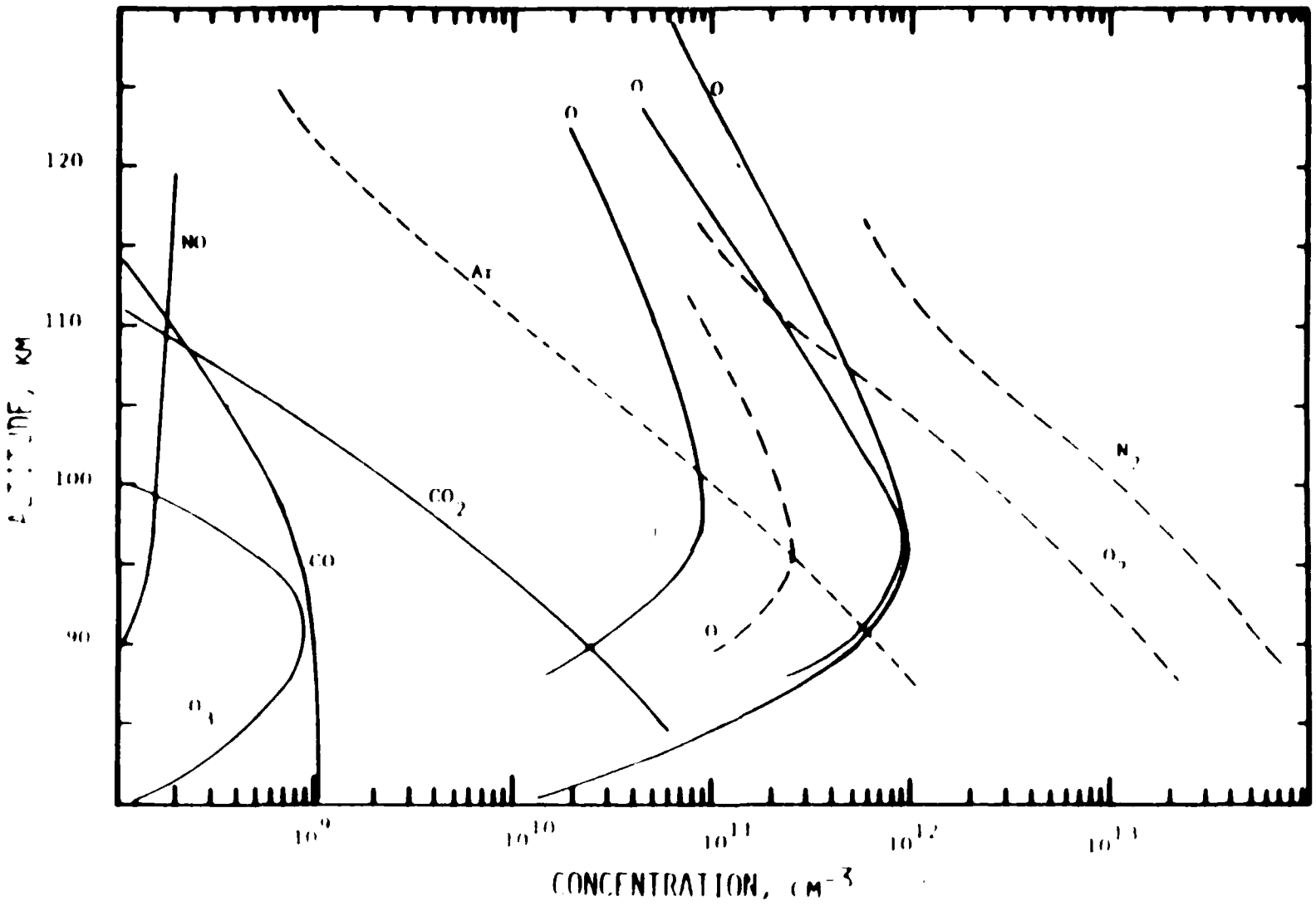

Figure 2.2 Atmospheric Concentration Profiles. Dashed lines for N_2, O_2, and O are model calculations from Reneshea et al. (Ref. 12). Solid lines for O are measurements from Refs. 13-15. Other species are Ar (Ref. 16), CO_2 and CO (Ref. 17), O_3 (Ref. 12), and NO (Ref. 18).

resonance excitation curves for N_2 and are thus "uncovered" by the dominant N_2 excitation process. Vibrational levels of CO higher than v = 4 will not be excited due to their overlap with the larger cross sections for the far more abundant N_2.

Measured electron impact cross sections for excitation to specific CO vibrational levels as presented in Reference 8 are plotted in Figure 2-3. Also presented for comparison is the total cross section for N_2 vibrational excitation from Reference 20.

The quantitive result of our modeling effort at 100 km was that 6×10^{-3} quanta of CO vibrational excitation would be created per ion pair with 84% of the excited CO created in v = 1, 10% in v = 2, 4% in v =3, and 2% in v = 4. This distribution arises from calculated vibrational energy distributions, N_v, ratios of 1.0/.12/.05/.02 with a CO mixing ratio of 5×10^{-5}. It should be noted that spectral fitting routines assuming N_v quite similar to these calculated values provide an excellent fit to the EXCEDE:SPECTRAL CVF data feature at 4.7 μm.[3]

The 6×10^{-3} quanta/ion pair is derived as follows:

Given the fact that higher vibrational levels of CO have radiative lifetimes approximated by $\tau(1 \rightarrow 0)/v$,[21] the immediate 4.7 μm output for the calculated 100 km N_v distribution is close to $\sum_{v=1}^{4} vN_v$ or ~1.5 times the v = 1 emission rate. Since the CO(v = 1) production rate was calculated to be 4×10^{-3} /ion pair at 100 km,[3] and since the steady state production and emission rates are equal, when correction is made for the faster radiative lifetimes of v = 2, 3, and 4, the "apparent" calculated emission rate is ~1.5 times higher or 6×10^{-3} per ion pair.

The Winick model was also used to predict a 3914Å band production/emission rate from N_2^+ of 6×10^{-2} quanta per ion pair, resulting in a predicted ratio of CO (4.7 μm) to N_2^+ (3914Å) steady state emission rate of ~0.006/0.06 or ~0.1. A plot of this ratio from the EXCEDE spectral data is shown as the open circles in Figure 2-4. Although there is

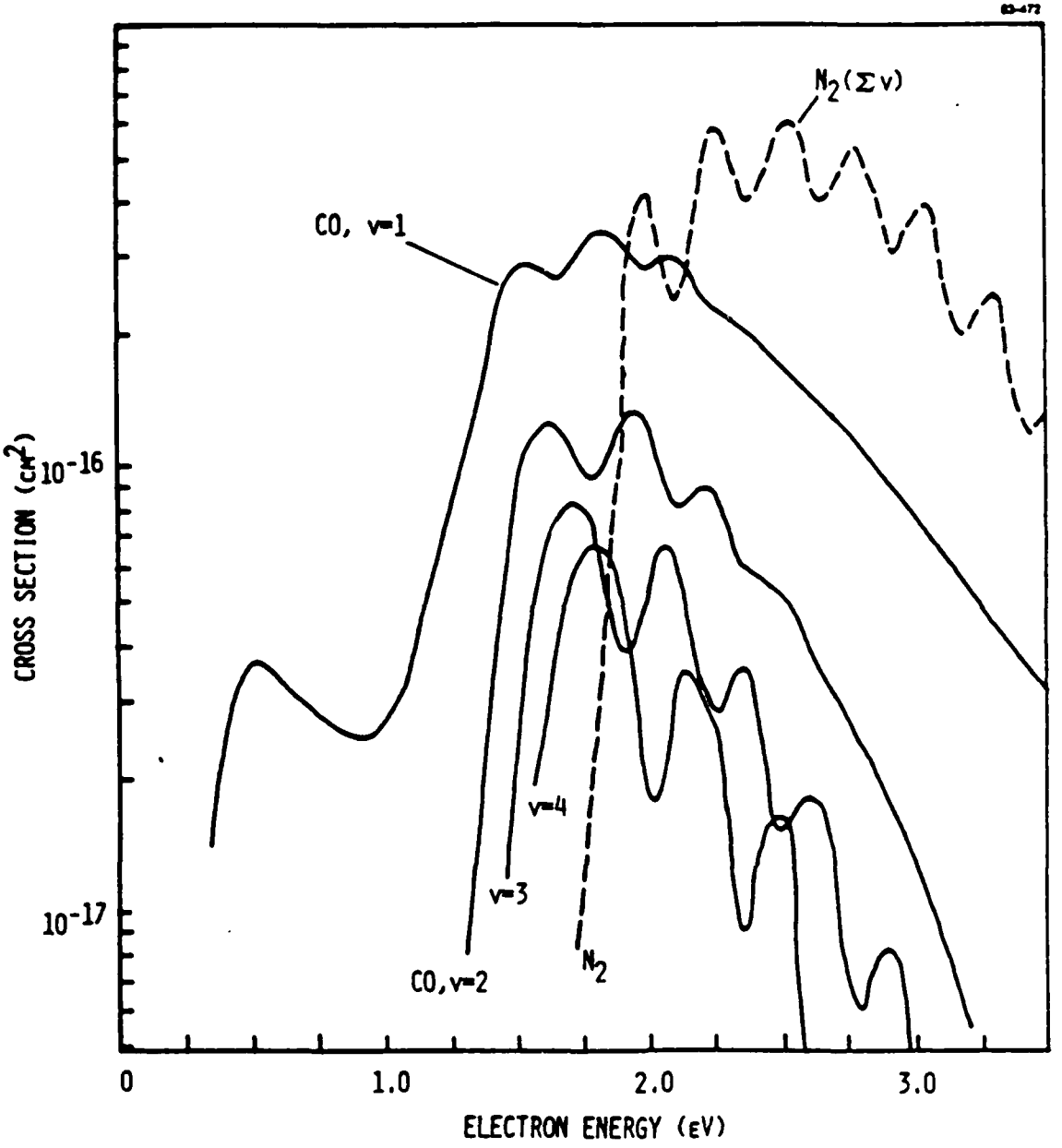

Figure 2-3. Vibrational Excitation Cross Sections for CO vibrational levels and for $N_2(\Sigma v)$

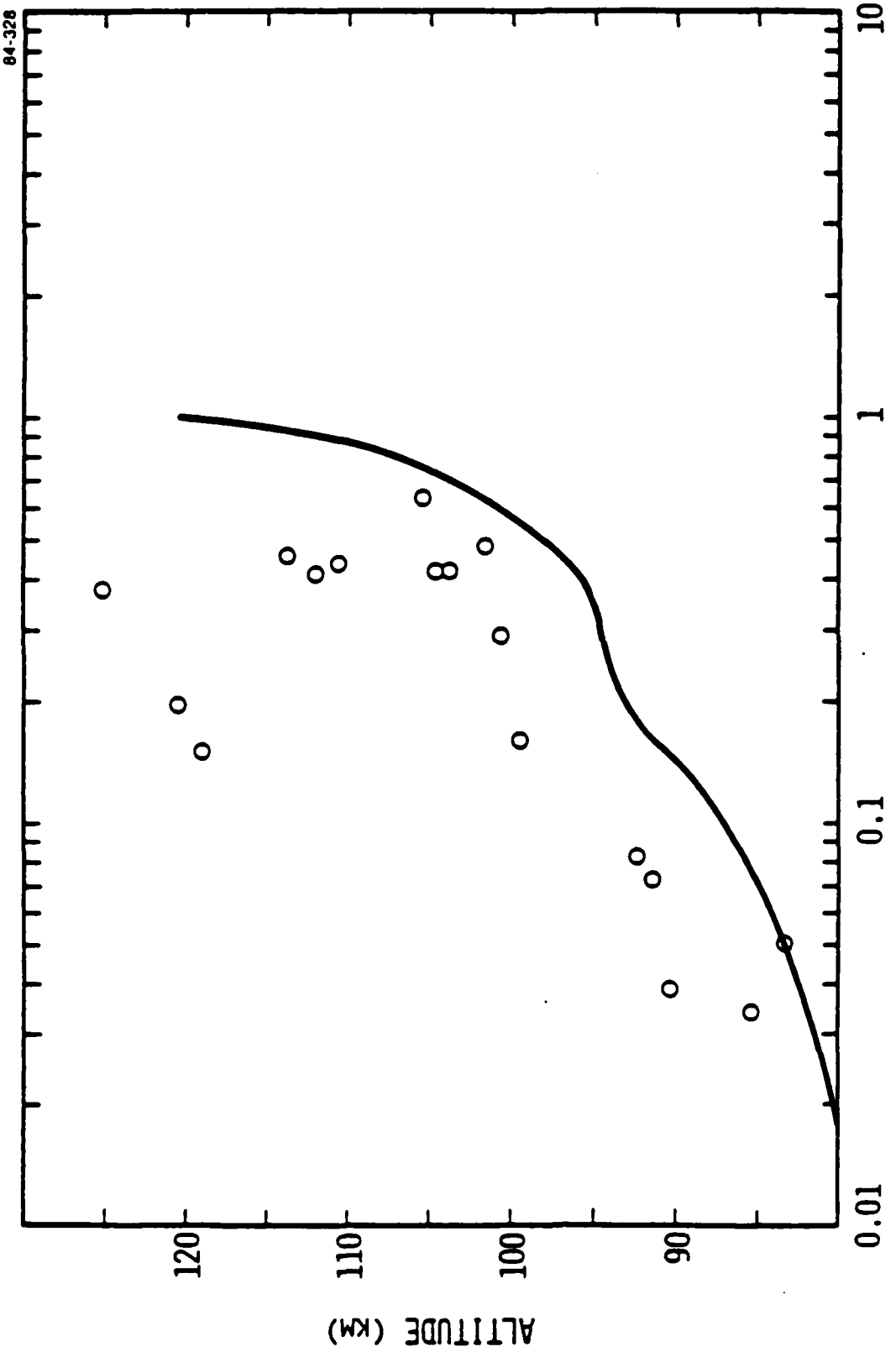

Figure 2-4. 4.7 μm/N_2^+ (3914) Intensity Ratio and CO Mixing Ratios (Ref. 7)

considerable scatter in the data, the two points nearest 100 km give I (4.7 μm)/I (3914Å) ratios of about 0.15 and 0.28 in good agreement with the calculated value of 0.1 given the considerable uncertainties in the model and its inputs.

Furthermore, given the model assumption that both CO vibrational excitation and N_2^+ (3914Å) production are direct electron impact processes we expect the altitude dependence of the I (4.7 μm)/I (3914Å) steady state emission to follow the CO mixing ratio profile which, in turn, is proportional to the CO/N_2 ratio. As illustrated in Figure 2-4 given the data scatter the CO mixing ratio is a good indicator of the I (4.7 μm)/I (3914Å) emission particularly between 95 and 110 km.

Thus, the spectral shape, absolute emission level and altitude profile of the EXCEDE:SPECTRAL 4.7 μm feature are all well explained by direct electron impact excitation of ambient CO. This unexpected result has been recently supported by the observation of high resolution CO spectra measured by the rocket borne Field Widened Interferometer experiment.[22]

In summary, as first presented in Reference 3, the steady state beam-on production of 4.7 μm radiation is well explained by invoking the direct excitation of CO by secondary electrons in the 1 to 2 eV range. Since the production rate of CO vibrational quanta is ~6×10^{-3} quanta per ion pair at 100 km, and since each quanta is about 0.26 eV, the fraction of beam energy deposited in CO vibration at 100 km is ~$6 \times 10^{-3} \times 0.26$ eV/35 eV or ~4.5×10^{-5} of the major energy deposition mechanism. As indicated by Figure 2-4, this energy deposition ratio probably rises by a factor of 2-3 in the 105 to 120 km range. The ratio of deposition energy to ion pair production energy will be a key indicator in the discussion of the temporal evolution of CO 4.7 μm radiation discussed in the following subsection.

2.2 Temporal Predictions for CO 4.7 μm Radiation

Infrared observations from the EXCEDE spectral mission[1,2] were limited to a region of active electron beam irradiated atmosphere interspersed with nonirradiated regions as the electron beam switched on and off. This experimental geometry favors "prompt" emitters which are directly excited by the incident electron flux and have radiative lifetimes shorter than the observation time as the onboard instruments' fields of view pass through the irradiated volume (~10 ms). It has been recognized that radiation due to secondary excitation processes (e.g., metastable E→V exchange or infrared chemiluminescence) and/or longer lived emitters could be better analyzed if future EXCEDE missions were designed to view post-irradiated regions where prompt emissions are decaying at a faster rate than radiation from secondary processes or even long-lived promptly excited states.

The following subsections are an attempt to review all relevant prompt and secondary CO vibrational excitation mechanisms, in terms of their strength (the ratio of expected deposition energy into CO vibrational states to the energy deposited into ion pair production) and characteristic production and decay times. This review is intended to identify the major CO(v) production mechanisms and their inherent time scales as an aid to predicting 4.7 μm radiation characteristics available for observation by future EXCEDE missions.

The potential CO(v) excitation mechanisms reviewed in this effort are listed in Table 2-1. The mechanisms reviewed include two direct processes: secondary electron excitation of ambient CO and dissociative excitation of ambient CO_2; and nine indirect processes, including intermolecular E→V quenching of the electronic metastable species $N_2(A)$, $O(^1S)$, $O(^1D)$, $O_2(b^1\Sigma)$, $O_2(a^1\Delta)$, and the 4.5 eV states of O_2, E→E quenching of $N_2(A)$ followed by secondary intramolecular E→V quenching of $CO(a^3\pi)$, V→V quenching of $N_2(v)$ and infrared chemiluminescence in the reaction of O^+ with CO_2.

The bulk of the indirect processes considered involve the intermolecular E→V quenching of electronically excited species. A summary of the excitation energy and major excitation and quenching processes of these metastable

electronic energy reservoir species is shown in Table 2-2. Production and loss mechanisms of several reservoir species for EXCEDE experimental conditions have been deduced from analysis of the PRECEDE experiment.[23,5] Other key excitation and loss mechanisms can be evaluated from the work of Torr and Torr.[24] An analysis of the potential role of both electronically and vibrationally excited reservoir species in the production of CO(v) is presented below.

Table 2-1 - Excitation Mechanisms for CO(v)

PROCESS FORMULA	PROCESS TYPE
1) $e + CO \rightarrow CO(v) + e$	Direct electron impact
2) $e + CO_2 \rightarrow CO(v) + O + e$	Electron impact dissociative excitation
3) $N_2(v) + CO \rightarrow CO(v') + N_2(v-v')$	V-V exchange with N_2
4) $N_2(A) + CO \rightarrow CO^*(a,v) + N_2$ $CO^*(a,v) \rightarrow CO(v') + h\nu$ $CO^*(a,v) + M \rightarrow CO(v') + N_2$	E-E exchange with $N_2(A)$ plus radiative or collisional quenching
5) $N_2(A) + CO \rightarrow CO(v) + M$	E-V exchange with $N_2(A)$
6) $O\ (^1S) + CO \rightarrow CO(v) + O\ (^3P)$	E-V exchange with $O\ (^1S)$
7) $O\ (^1D) + CO \rightarrow CO(v) + O\ (^3P)$	E-V exchange with $O\ (^1D)$
8) $O_2\ (c,A,A') + CO \rightarrow CO(v) + O_2$	E-V exchange with O_2^*
9) $O_2\ (b^1\Sigma) + CO \rightarrow CO(v) + O_2$	E-V exchange with O_2^*
10) $O_2\ (a^1\Delta) + CO \rightarrow CO(v) + O_2$	E-V exchange with O_2^*
11) $CO_2 + O^+ \rightarrow CO(v) + O_2^+$	Infrared chemiluminescence

Table 2-2 - Electronically Metastable Reservoir Species

EXCITED SPECIES	EXCITATION ENERGY (eV)	RADIATIVE LIFETIME (sec)	MAJOR EXCEDE PRODUCTION MECHANISMS	MAJOR LOSS MECHANISMS
N_2 ($A\ ^3\Sigma^+$)	6.16	~2	$e + N_2 \rightarrow N_2(A,B,C,etc.)$	$N_2(A) + O$
			$N_2(B,C,etc.) \rightarrow N_2(A) + h\nu$	$N_2(A) + O_2$
$O(^1S)$	4.19	.9	$N_2(A) + O$	$O(^1S) + O_2$
			$O_2^+ + e$	$O(^1S) \rightarrow O(^1D) + h\upsilon$
			$e + O$	
$O(^1D)$	1.97	110	$O_2^+ + e$	$O(^1D) + N_2$
			$e + O$	$O(^1D) + O_2$
			$O(^1S) \rightarrow O(^1D) + h\nu$	
O_2 $A\ ^3\Sigma_u^+$,	4.5-5.0	0.18	$e + O_2$	$O_2^* + O$
$A'\ ^3\Delta_u$		5-50	$N_2(A) + O_2$	$O_2^* + N_2$
$c\ ^1\Sigma_u^-$		25-50		$O_2^* \rightarrow O_2 + h\nu$
O_2 ($b\ ^1\Sigma_g^+$)	1.64	12	$e + O_2$	$O_2(b) + N_2$
			$O\ (^1D) + O_2$	$O_2\ (b) \rightarrow O_2(a) + h\nu$
			$O\ (^1S) + O_2$	
O_2 ($a\ ^1\Delta_g$)	0.98	2700	$e + O_2$	$O_2(a) + O_2$
			$O_2(c,A') + h\upsilon$	
			$O_2(b) + h\upsilon$	
CO ($a\ ^3\pi$)	6.01	~.007	$e + CO$	$CO(a) + N_2$
			$N_2(A) + CO$	$CO(a) \rightarrow CO + h\nu$

2.2.1 Direct Electron Impact Excitation of CO

As reviewed in Section 2-1 our previous analysis of the EXCEDE:SPECTRAL Mission identified direct electron impact on ambient CO as the predominant mechanism for the production of "prompt" CO(v).[3] Our model analysis for the 100 km case (5×10^{-5} mixing ratio for CO) predicted the amount of beam energy deposited in CO(v) was ~4.5×10^{-5} of the ion pair creation energy.

The infrared emission time scale associated with this direct excitation mechanism is the intrinsic radiative lifetime of the CO(v) excited states. The radiative emission time scale dominates because the quenching of low CO(v) states by atmospheric species is very slow. For example the rate constant at 300°K for V = 1 state of CO to undergo V→V exchange with N_2 is 5×10^{-16} cm^3 sec^{-1}, with O_2 it is 9×10^{-17} and the V→T/R rate constant for Ar is less than 3×10^{-18}.[25] For vibrational quenching to compete with radiative decay at 100 km where the N_2 number density is 10^{13} cm^{-3}, the quenching rate constant, K_Q, for N_2 would have to exceed 3×10^{-12} since:

$$k_Q[M] \geq 1/\tau_{rad} = 35 \text{ sec}^{-1}.$$

The V→T/R rate for atomic oxygen would have to exceed 3×10^{-11}, and although room temperature rates are not available for this process it is unlikely that O is more than 10^7 times more effective than the upper limit for Ar.

A best estimate of the CO(v=1) radiative lifetime is 28.3 msec based on four recent determinations of the CO(1→0) integrated band absorption coefficient of 266.0,[26] 282.2,[27] 279[28] and 273[29] cm^{-2} atm^{-1} at standard temperature and pressure.

Averaging these four values gives an integrated band intensity, S, of 275 cm^{-2} atm^{-1} (STP). Using Penner's expression relating $S_{\ell u}$ with the radiative lifetime[30] and a band center frequency, $\upsilon_{\ell u}$, of 2143 cm^{-1} or 6.42×10^{13} sec^{-1} yields:

$$\tau_{rad}(1\rightarrow 0) = \frac{3.21 \times 10^{28}}{S_{\ell u}\, \upsilon_{\ell u}^{2}} = \frac{3.2 \times 10^{28}}{275 \times (6.42 \times 10^{13})^{2}} = .0283 \text{ sec}$$

Thus the direct excitation of CO(v) by electron impact will decay after beam termination with a rate constant of $1/\tau_{rad} = A\ (1\rightarrow 0) = 35\ sec^{-1}$ for v = 1, with higher vibrational levels displaying a radiative decay rate approximately v times A $(1\rightarrow 0)$[21] cascading to lower v's. However, since we have calculated[3] that for the 100 km case 84% of the excited CO will be created in v = 1 the 35 sec^{-1} decay rate constant will dominate the 4.7 μm fall off from direct excitation.

In summary, for our 100 km benchmark altitude with a CO mixing ratio of 5 x 10^{-5}, we predict that about 4.5 x 10^{-5} of the ion pair creation energy will be deposited by direct electron impact excitation into the CO vibrational manifold, with the great bulk of the excitation in v = 1. This radiative source will start coincident with the exciting electron deposition and the predominant component will decay after beam termination at the radiative decay rate of the v = 1 component with a decay rate constant of 35 sec^{-1}.

2.2.2 Dissociative Excitation of Carbon Dioxide

As shown in Figures 1-2 and 2-2 the ambient CO_2 concentration exceeds that of CO by about a factor of 3 at 100 km, equals the CO concentration near 108 km and falls below the CO concentration at altitudes above 108 km.

Since the O-CO bond energy in CO_2 is 5.5 eV, electrons with energy in excess of about 5.75 eV are capable of dissociating CO_2 and leaving the CO fragment vibrationally excited. If the dissociating electron attaches to the atomic oxygen, the energy dissociation threshold is lowered to 4.0 eV with ~4.25 eV required for CO vibrational excitation.

There are no cross section measurements available which indicate the degree of CO vibrational excitation in direct dissociation or dissociative attachment electron impact cross sections for CO_2. However, in both neutral and ionic chemical reactions there is a general observation that vibrational

reaction energy is usually not present in a molecular fragment unless it is formed during the reaction. Thus for an exothermic reaction of the type

$$ABC + D \rightarrow AB + CD$$

the fragment CD which is formed in the reactive process if far more likely to be excited than the AB fragment.

By analogy, we might expect that the electron impact processes:

$$e + CO_2 \begin{cases} \rightarrow CO + O^- \\ \rightarrow CO + O + e \end{cases}$$

might not be particularly effective means of producing vibrationally excited CO.

Cross sections are available for the dissociative attachment portion of the process noted above with the room temperature value displaying two narrow (~1eV) peaks (with no observable vibrational structure) reaching ~1.5 x 10^{-19} cm^2 just above 4 eV and ~4.5 x 10^{-19} just above 8 eV.[20] This can be compared with the total direct excitation cross section for CO(v) (individual vibrational level cross sections are shown in Figure 2-3) which peaks above 8 x 10^{-16} cm^{-2}.[19,20] Electron energy loss in the 4 and 8 eV ranges is dominated by momentum transfer to N_2 ($\sigma \approx 10^{-15}$ cm^2)[20] and possibly by electronic excitation of O_2 and N_2 respectively.

However, even the first mechanism, momentum transfer to N_2, would dominate CO_2 dissociation as an energy loss mechanism in the 4 and 8 eV ranges. This can be seen from a simple comparison of energy loss for the two processes. The momentum transfer energy loss fraction can be approximated by the ratio of the electron to N_2 mass of 2 x 10^{-5} multiplied by the electron energy (4 or 8 eV, corresponding to the two peaks in the CO_2 dissociation cross section). Thus the 4 eV energy loss rate for momentum transfer to N_2 at 100 km can be approximated by:

$$R_{N_2} \approx v_e \, \sigma_{N_2} \, [N_2] \, \Delta E$$

$$\approx v_e \text{cm sec}^{-1} \times (10^{-15} \text{ cm}^2) \times (10^{13} \text{ cm}^{-3}) \times (4 \text{ eV}) \times 1 \times 10^{-5}$$

$$\approx 8 \times 10^{-7} \, (v_e) \text{ eV/sec}$$

while the comparable energy loss rate for CO_2 dissociation is

$$R_{CO_2} = v_e \, \sigma_{CO_2} \, [CO_2] \, \Delta E$$

$$= v_e \text{ cm sec}^{-1} \times (1.5 \times 10^{-19} \text{ cm}^2) \times (3 \times 10^9 \text{ cm}^{-3}) \times (4 \text{ eV})$$

$$= 1.8 \times 10^{-9} \, (v_e) \text{ eV/sec}$$

Thus, the energy loss rate ratio for CO_2 dissociation and N_2 momentum transfer at 4 eV is less than $1.8 \times 10^{-9} \, v_e \, / \, 8 \times 10^{-7} \, v_e$ or 1/400 of the loss rate for momentum transfer to N_2. A similar fraction applies at the 8 eV resonance peak as well. Since we have argued that probably only a small fraction of the dissociative attachment events leave the CO fragment vibrationally excited, and since most of the energy loss in the CO_2 process is taken up in breaking the CO_2 bond not exciting CO(v), it seems probable that CO(v) production from CO_2 cannot compete with direct excitation of CO. This is particularly true of altitudes above 108 km where CO is more abundant than CO_2 to start with.

If CO(v) production from CO_2 were comparable with direct excitation of CO, the 4.7 μm radiation feature observed in the EXCEDE:Spectral experiment should have followed the CO_2 mixing ratio profile, at least in the 90-105 km region where $[CO_2] > [CO]$ (see Figure 2-1). As illustrated in Figure 2-4 the 4.7 μm profile appears to closely follow the CO mixing ratio (sharply increasing between 90 and 100 km and constant in the 100-115 km range) not the monotonically decreasing CO_2 mixing ratio. This strongly corroborates our

argument that CO_2 dissociation is a minor source of CO(v) under EXCEDE conditions.

Of course any CO(v) created by impact dissociation of CO_2 would decay with the same radiative quenching rate characteristic of directly excited CO upon beam termination.

2.2.3 Vibrational Exchange with $N_2(v)$

As indicated by the large electron impact cross section for vibrational excitation of N_2 plotted in Figure 2-3 and the fact that N_2 is the dominant atmospheric species in the 90-120 km range as shown in Figure 2-2, the EXCEDE experiments can be expected to produce copious amounts of $N_2(v)$. Since $N_2(v)$ does not have an electric dipole moment it forms a long lived metastable energy source until collisionally quenched. The principal quenchant for $N_2(v)$ by the altitude range of interest is atomic oxygen with a quenching rate constant of ~2 x 10^{-15} cm^3 sec^{-1} for N_2 (v = 1) at upper mesopheric and lower thermospheric temperatures.

Given an atomic oxygen density at 100 km of 8 x 10^{10} to 8 x 10^{11} cm^{-3} from Figure 2-2 this corresponds to a $N_2(v)$ quenching rate of between 1.6 x 10^{-4} and 1.6 x 10^{-3} sec^{-1} or a quenching lifetime of greater than 625 sec. (or 10 minutes) at 100 km. Thus, for any time scale of interest to an on board or fly along EXCEDE experiment the $N_2(v)$ pool will remain constant.

The rate constant for the production of CO (v = 1) from N_2 (v = 1) at temperatures characteristic of 100 km is about 8 x 10^{-15} cm^3 sec^{-1}.[31] Thus, the time scale for the production of CO(v) from $N_2(v)$ is also quite long. Assuming $[CO] \ll [N_2(v)]$ and a CO concentration of 5 x 10^8 at 100 km (from Figure 2-2) then the rate for the production of CO(v) is 8 x 10^{-15} cm^3 sec^{-1} x 5 x 10^8 cm^{-3} = 4 x 10^{-6} sec^{-1} giving a V-V exchange time scale 2.5 x 10^5 seconds or almost 3 days.

The fraction of the beam energy directly deposited into $N_2(v)$ is probably well approximated by the ~2.0 eV slice between ~ 1.6 and 3.6 eV electron energy range which is dominated by the N_2 shape resonance plotted in

Figure 2-3. In this energy range $N_2(v)$ excitation dominates energy loss processes. This direct excitation also dominates total $N_2(v)$ production although some additional $N_2(v)$ production through O^1D and O_2^* quenching will also occur. Since the electron energy loss per ion pair is 35 eV, each secondary electron loses roughly 2/35 or 6% of its energy to direct excitation of $N_2(v)$. This estimate is in agreement with Winnick's model at 100 km which predicts that 8.7% of the ion pair creation energy is deposited in $N_2(v)$. If roughly 6×10^{-4} of the ion pair formation energy is present as $N_2(v)$, then the fraction flowing into CO(v) is limited by the ratio of CO to O quenching of $N_2(v)$ which at least for $N_2(v = 1)$ can be estimated.

If we take the CO_2 and O at 100 km to be 5×10^{-7} and 5×10^{-3} respectively then the ratio of their $N_2(v = 1)$ quenching rates is

$$k_{CO_2}[CO_2]/k_O[O] = ((3.8 \times 10^{-13}) \times (5 \times 10^{-7}) / (2.2 \times 10^{-11}) \times (5 \times 10^{-3})$$

$$= 4 \times 10^{-3}$$

Thus, the fraction of the ion pair creation energy deposited through $N_2(v)$ into CO(v) can be estimated as $6 \times 10^{-4} \times 4 \times 10^{-3}$ or 2.4×10^{-6}.

This level of fractional energy tranfer is about 5 times greater than the 4.5×10^{-5} fraction calculated for direct CO excitation at 100 km. However, it is important to remember that the deposition rate is very slow compared with the direct process. The direct process is fast enough to reach steady state when the beam is on and decays with the CO radiative lifetime of 28.5 msec. The $N_2(v)$ process pumps energy into CO(v) with a time scale that is very long compared to the beam-on duration and decays with $N_2(v)$ quenching by O-atoms on a time scale of roughly 10 minutes.

By dividing total energy input fraction by the decay time constants for each process we can assess their initial relative radiative output rates

$$N_2(v): \quad \frac{2.4 \times 10^{-6}}{625 \text{ sec}} = 3.8 \times 10^{-9}$$

$$e + CO: \quad \frac{4.5 \times 10^{-5}}{0.0283 \text{ sec}} = 1.6 \times 10^{-3}$$

Thus, initially the direct excitation mechanism is a 4 x 10^3 stronger source of CO(v) radiation; however, after ~9 radiative lifetimes (0.25 s) the direct source will decay to a point where the $N_2(v)$ source dominates. The $N_2(v)$ source will then dominate until the $N_2(v)$ is quenched, a process which will require several tens of minutes.

2.2.4 Quenching of Metastable Electronic States

Analysis of the first three CO(v) excitation mechanisms listed in Table 2-1 has shown that process (1), the direct electron impact excitation of CO will be the dominate source of CO(v) radiation while the beam is on and will decay exponentially until dominated after roughly 0.25 s by process 3, the V-V exchange with N_2.

The purpose of this subsection is to investigate processes 4 through 10 from Table 2-1, all of which involve the quenching of electronically metastable species which may be directly or secondarily created by electron impact. Key characteristics of these metastable states are summarized in Table 2-2.

Mechanisms 4 and 5 involve quenching of $N_2(A)$. Under EXCEDE conditions the production of N_2 A has been estimated to be equivalent to the ion pair production rate.[31] Since each $N_2(A)$ represents at least 6.16 eV of excitation energy, over 17% of the ion pair production energy appears to flow through this species. Mechanism 4 from Table 2-1 is a two step process whereby $N_2(A)$ is quenched by O to form the CO(a) state in a near resonant E-E exchange process. CO(a) is then collisionally or radiatively quenched to yield CO(v). Mechanism 5 involves direct E-V quenching by CO.

As indicated by Table 2-2, $N_2(A)$ is rapidly reactively destroyed by O and O_2 with $N_2(A)$, with v = 0 rate constants of 3 x 10^{-11} cm^3/sec[32] and 2 x 10^{-12} respectively.[33] If we take $[O]$ at 100 km to be 5 x 10^{12} cm^{-3} and $[O_2]$ as 4 x

10^{12} cm^3 then the quenching rate for $N_2(A)$ is:

$$Q_{O + O_2} = k_O[O] + k_{O_2}[O_2] = 3 \times 10^{-11} \times 5 \times 10^{11} +$$

$$2 \times 10^{-12} \times 2 \times 10^{12} = 19 \text{ sec}^{-1}$$

which is significantly faster than the compared radiative quenching rate of $1/\tau_{rad} = 0.5$ sec^{-1}.

The quenching rate constant for $N_2(A)$, $v = 0$ by CO is 5×10^{-12}. For a [CO] of 5×10^8 at 100 km the CO quenching rate:

$$Q_{CO} = k_{CO}[CO] = 5 \times 10^{-12} \times 5 \times 10^8 = 2.5 \times 10^{-3} \text{ sec}^{-1}$$

which is 1.3×10^{-4} of the combined O and O_2 rate. The amount of $N_2(A)$ energy eventually deposited in CO(v) when CO quenches $N_2(A)$ is not known, but since most of the reaction passes through CO(a) which will radiatively decay at a rate of ~140 sec^{-1} it may be quite small. This fraction of the ion pair energy flowing into CO(v) via $N_2(A)$ can be written as the fraction of the ion pair energy going to $N_2(A)$ (.17) times the fraction quenched by CO (2×10^{-4}) times the fraction of the energy quenched ending up as CO(v). If we take this latter fraction, designated $f_v(CO)$, as certainly 0.1 or less we then estimate that mechanisms 4 and 5 together cannot pump more than $0.17 \times 2 \times 10^{-4} \times 0.1$ or 3.4×10^{-6} of the ion pair energy. This fraction is significantly less than the 4.5×10^{-5} calculated for direct excitation, but might play a role after a few radiative decays of the directly excited CO(v) - if $f_v(CO)$ is as large as 0.1 for the combination of processes 4 and 5.

$O(^1S)$ quenching by CO is a second potential E→V source of CO(v). As shown in Table 2-2 $O(^1S)$ is produced by atomic oxygen quenching of $N_2(A)$ and by dissociative neutralization of O_2^+. Since we have shown above that (depending on [O] assumed) roughly half of the $N_2(A)$ at 100 km is quenched by

0. Recent measurements indicate that .75% of these quenching interactions result in $O(^1S)$ production.[35] Thus at 100 km roughly 0.4 $O(^1S)$ per ion pair may be created through the $N_2(A)$ channel. Analysis of the PRECEDE experiment indicated that this mechanism dominates $O(^1S)$ production under EXCEDE-like conditions in the 100-116 km range with O_2^+ recombination dominating only below 96 km.[23] Assuming the $N_2(A)$ source is dominant at 100 km the fraction of the ion pair production energy flowing through $O(^1S)$ is the $O(^1S)$ energy as a fraction of the ion pair energy (4.19/35 eV) times 0.4 or ~0.05.

As shown in Table 2-2 the main deactivation mechanisms for $O(^1S)$ are quenching by O_2 and radiative decay. Previous laboratory experiments indicating a fast quenching rate for $O(^3P)$ have been discredited due to $O_2(^1\Delta)$ contamination results obtained since the analysis of the PRECEDE experiment[23] was published. The quenching rate constant for O_2 has been measured as 3.6×10^{-13} cm^3 sec^{-1}.[36] For a 100 km $[O_2]$ of 4×10^{12} cm^{-3} this leads to a quenching rate of:

$$Q_{O_2} = k_{O_2} [O_2] = 3.6 \times 10^{-13} \times 2 \times 10^{12} = 0.7 \text{ sec}^{-1}$$

which is slightly slower than the radiative quenching of $1/\tau_{rad} = 1.1$ sec^{-1}. Taken together, the O_2 and radiative quenching rate can be estimated as ~1.8 sec^{-1} at 100 km. The quenching of $O(^1S)$ by CO is an inefficient process with a measured rate constant of 4.9×10^{-15} cm^3 sec^{-1}.[36] Assuming a $[CO]$ of 5×10^8 cm^{-3} leads to a $O(^1S)$ quenching rate by CO of:

$$Q_{CO} = k_{CO} [CO] = 5 \times 10^8 \times 4.9 \times 10^{-15} = 2.5 \times 10^{-6} \text{ sec}^{-1}$$

Thus, at 100 km the $O(^1S)$ quenching rate by CO is estimated to account for no more than 2.6×10^{-6} $sec^{-1}/1.8$ $sec^{-1} \approx 1.4 \times 10^{-6}$. Since $O(^1S)$ represents 0.05 of the ion pair creation energy, the $O(^1S)$ source can not channel more than a negligible ~ 7×10^{-8} of the ion pair production energy into CO(v).

The third possible source of CO(v) by E→V exchange from metastable electronic species is $O(^1D)$. From Table 2-2 $O(^1D)$ can be produced by dissociative recombination of O_2 and NO^+ and also by radiative quenching of $O(^1S)$. Since the neutralization of both O_2^+ and NO^+ efficiently produce $O(^1D)$ and since N_2^+ produces either NO^+ or O_2^+ in interaction with O and O_2 respectively the ion channel may produce nearly one $O(^1D)$ per ion pair through dissociative neutralization.

For the $O(^1S)$ channel, nearly 96% of the radiatively damped $O(^1S)$ produces $O(^1D)$[24] and since at 100 km we have estimated that ~44% of the $O(^1S)$ quenches radiatively, then we expect roughly 0.96 x 0.44 x 0.4 = 0.17 $O(^1D)$ per ion pair through the 0.4 $O(^1S)$ per ion pair as observed in the PRECEDE experiment. Thus in total we expect ~1.17 $O(^1D)$ per ion pair representing 1.17 x $E(O^1D)/E$ (Ion Pair) = 1.17 x 1.97/35 = 0.066 of the ion pair production energy.

The main quenching mechanism for $O(^1D)$ at 100 km is quenching by N_2 with a quenching rate constant of 2.3×10^{-11} cm^3 sec^{-1}.[24] The rate constant for O_2 quenching is a factor of 1.5 to 3 larger than that for N_2,[24] but the concentration of N_2 is 5 to 10 times the O_2 concentration at the altitudes of interest leaving N_2 as the dominate quencher.

At 100 km, the combined N_2 and O_2 quenching rate can be calculated. After choosing the laboratory measured rate for O_2 quenching of 3.6×10^{-11} cm^3 sec^{-1} [24] we calculate:

$$Q_{N_2 + O_2} = k_{N_2}[N_2] + k_{O_2}[O_2]$$

$$= 2.3 \times 10^{-11} \times 1 \times 10^{13} + 3.6 \times 10^{-11} \times 2 \times 10^{12}$$

$$= 300 \text{ sec}^{-1}$$

The total rate constant for CO quenching of $O(^1D)$ has been measured as 7.3×10^{-11} cm^3 sec^{-1} with a vibrationally specific rate constants (ratioed to 1.0

for v = 1) of: 1.5, 1.0, 0.66, 0.50, 0.36, 0.25, 0.12, 0.011 for V = 0 to 7 respectively.[37] This yields an average CO(v) of 1.7. The quenching rate of $O(^1D)$ to CO at 100 km is then:

$$Q_{CO} = k_{CO} [CO] = 7.3 \times 10^{-11} \times 5 \times 10^{8}$$

$$= 3.7 \times 10^{-2} \text{ sec}^{-1}$$

When compared with the N_2 and O_2 rate of 3×10^2 we predict that $\approx 1.2 \times 10^{-4}$ of the $O(^1D)$ energy or $1.2 \times 10^{-4} \times 0.066 = 7.9 \times 10^{-6}$ of the ion pair production energy will be deposited in CO through $O(^1D)$ quenching at 100 km. This $\sim 8 \times 10^{-6}$ is fairly small (~1/6) compared to the 4.5×10^{-5} calculated for direct electron impact excitation at 100 km and since the $O(^1D)$ source is collisionally quenched with a time constant of $1/3.0 \times 10^2$ sec^{-1} = 3 msec this source does not significantly outlast the direct excitation channel. However, within the uncertainties of the respective estimates it may noticeably enhance the direct electron impact excitation source.

The final metastable reservoir species to be considered are all electronically excited states of molecular oxygen. They include three highly excited states in the 4.5 to 5 eV range and the lower lying and better characterized b $^1\Sigma_g^+$ and a $^1\Delta g$ states. Key characteristics for these states are listed in Table 2-2.

Our previous analysis of the PRECEDE long lived visible and near ultraviolet 4.5 glow identified the three 4.5-5.0 eV O_2 states as probable important species under EXCEDE excitation conditions and reviewed apparent observations of these states in the natural aurora and airglow. The integrated strength of the long lived PRECEDE glow represents 5-6% of the beam deposition energy and represents an average $[O_2^*]$ in the irradiated volumes of order $10^7 - 10^8$ cm^{-3}.

Quenching data for the three 4.5-5 eV O_2 states is scarce, but recent studies by Kenner and Ogryzlo have yielded room temperature values of 9.3×10^{-15}, 1.3×10^{-11}, 1.3×10^{-13}, 7×10^{-13} and 7.2×10^{-16} for $O_2(A)$ quenching

by N_2, O, O_2, CO_2 and Ar respectively and 5.9×10^{-12}, 3×10^{-14}, $<6 \times 10^{-14}$, and 6×10^{-16} for $O_2(c)$ by O, O_2, CO_2 and Ar respectively.[38,39] The $O_2(A)$ values for O, O_2 and Ar are for the V = 2 state while other values are for the ground vibrational state. Except for the atomic oxygen values all of these rates are extremely slow and are consistent with our analysis of the PRECEDE data which indicates little quenching above 95 km. Atomic oxygen is probably the most serious quenchant above 95 km. If Kenner's and Ogryzlo's value of 5.9×10^{-12} for k_O is accepted for the $O_2(c)$ state then the quenching rate at 100 km, assuming [O] of 5×10^{11} cm^{-3}, is:

$$Q_O = k_O [O] = 5.9 \times 10^{-12} \times 5 \times 10^{11} = 3.0 \text{ sec}^{-1}$$

This compares with an expected radiative quenching rate of $1/\tau_{rad} = 0.04$ to 0.02 sec^{-1} from Table 2-2. However, it is important to remember that, as indicated in Figure 2.2, the atomic oxygen concentration is quite uncertain in this altitude range and also that the quenching rate constants results by Kenner and Ogryzlo are difficult to measure and have not been confirmed by either additional laboratory or field measurements.

No quenching rates for the 4.5-5 eV O_2 states are available for CO, however the rates for the isoelectronic species N_2 or CO_2 should certainly be indicative. A value in the 10^{-13} to 10^{-14} range seems most likely from the available data. Assuming a k_{CO} of 10^{-13} for all three states and a [CO] of 5×10^8 gives:

$$Q_{CO} = k_{CO} [CO] = 10^{-13} \times 5 \times 10^8 = 5 \times 10^{-5} \text{ sec}^{-1}$$

Comparing this number with the radiative quenching rates of 5.5, 0.2-0.02 and 0.04-0.02 for the A, A' and c states respectively indicates that no more than 10^{-5}, $2.5 \times 10^{-2 \text{to} 3}$ and $2.5\text{-}1.2 \times 10^{-2}$ of each state can be transferred from O_2^* to CO, this fraction is lessened by any collisional quenching of O_2^* energy which is not transferred into CO vibration. Assuming that 6% of the

incident beam is deposited in O_2*[5] allows probable upper bounds of CO(v) of 6 x 10^{-7}, 1.5 x 10^{-3} to 10^{-4}, and 1.5 to 0.7 x 10^{-3} of the beam energy for the A, A' and c states respectively.

While these probable upper limits are large, it is important to note that upper bounds or probable upper bounds have been assumed for k_{CO}, the fraction of E→V energy transfer from O_2^* to CO while lower bounds have been assumed for collisional quenching of O_2^*. All of these assumptions maximize the calculated limits on O_2^* to CO(v) E→V transfer and each could contribute at least a factor of 10 to the overestimate.

If none of these parameters are poorly estimated then the A' and c states of O_2^* might compete with $N_2(v)$ as a source of CO(v) decaying with a 5 to 50 second timescale (assuming radiative quenching predominates) compared with the 10 minute decay rate of $N_2(v)$. Due to its faster radiative and collisional quenching rate the $O_2(A)$ state is clearly a negligible source of CO(v).

The two lower lying O_2 metastable electronic states, $O_2(b^1\Sigma_g^+)$ and O_2 ($a\,^1\Delta_g$) at 1.64 and 0.98 eV of energy represent the lowest energy electronic metastables from Table 2-1. Both the collisional and radiative quenching of these states is very slow and have been reviewed by Davidson and Ogryzlo;[40] the recommended quenching rate for $O_2(b)$ by N_2 is 2.2 x 10^{-15} cm^3 sec^{-1} and by CO is 3.3 x 10^{-15}. Since the $[CO]/[N_2]$ ratio is $[5 \times 10^8]/[10^{13}] = 5 \times 10^{-5}$ while the ratio of quenching rate constants is only 3.3 x 10^{-15}/2.2 x 10^{-15} = 1.5 it is clear that less than 1.5 x 5 x 10^{-5} ≈ 7.5 x 10^{-5} of the energy in $O_2(b)$ can flow through CO. However, at 100 km even the N_2 quenching rate:

$$Q_{N_2} = k_{N_2} [N_2] = 2.2 \times 10^{-15} \times 10^{13} = 2.2 \times 10^{-2} \text{ sec}^{-1}$$

is slow compared to the radiative quenching rate $1/\tau_{rad}$ = 1/12 sec = 8.3 x 10^{-2} sec, so less than 7.5 x 10^{-5} of the $O_2(^1\Sigma)$ energy passes through CO.

Given the excitation mechanisms (direct excitation by electron impact and $O(^1S)$ quenching by O_2 listed in Table 2-2) no more than 1% of the ion pair excitation energy can be expected to flow through $O_2(b)$. Thus, no more than

7.5×10^{-7} of the ion pair energy, a negligible amount, can reach CO(v) through this channel.

We also expect that $O_2(a)$ represents a negligible source of CO(v). While there appears to be no direct measurement of the CO quenching rate constant of $O_2(a)$, by analogy with $O_2(b)$, it can be expected to be similar to that for N_2. Since the O_2 quenching rate constant for O_2 is ~24 times larger than that for N_2, CO will probably have to compete with O_2 quenching as well as N_2 ($k_{O_2} = 2 \times 10^{-18}$). Since the $[CO]/[O_2]$ ratio at 100 km is $\sim 5 \times 10^8 / 2 \times 10^{12} \approx 2.5 \times 10^{-4}$ and the rate constant ratio can be expected to be about 1/24, the fraction of $O_2(a)$ quenched by CO compared with O_2 is about 10^{-5}. Given the sources of $O_2(a)$ listed in Table 2-2 (direct electron impact excitation and radiative decay from the c, A' and b states of O_2 we would not expect more than a few percent of the ion pair creation energy to pass through $O_2(a)$. Thus, the maximum energy fraction deposited into CO(v) by quenching of $O_2(a)$ is of order 10^{-7} which is negligible compared to other long lived sources.

2.2.5 Chemiluminescent Reaction Sources of CO(v)

Infrared chemiluminescent processes are known to play an important role in the production of many vibrationally excited species in the upper atmosphere. Thus, a systematic evaluation of exothermic reactions to produce CO(v) was undertaken. Since there is no apparent source of atomic carbon to form CO by oxygen abstraction or recombination, the only apparent chemical pathways to CO involve the abstraction of an oxygen atom from CO_2.

However, as noted in subsection 2.2.1 the O-CO bond is strong and furthermore any reaction as simple as an O atom extraction from CO_2 may well leave the nonparticipating CO fragment vibrationally cold. One potential chemiluminescent reaction which does produce CO in an exothermic process was identified, the reaction of O^+ with CO_2:

$$O^+ + CO_2 \rightarrow O_2^+ + CO$$

which is 1.5 eV exothermic and proceeds with a room temperature rate of 1.2×10^{-9} cm^3 sec^{-1}.[41]

The major source of O^+ is expected to be dissociative ionization of O_2 by electron impact a process which has about 1/3 the total ionization cross section for O_2,[20] thus about 1/3 of the O_2 ionized will form O^+.

Since $[O_2]$ is about 0.2 $[N_2]$ at 100 km and since the O_2 and N_2 total ionization cross sections are quite similar, we can estimate that O^+ is produced in about (1/3 x 1/6 = 1/18) or ~5% of the total ion pair production rate.

In addition to reacting with CO_2, the O^+ will react with N_2($k = 1.2 \times 10^{-12}$ cm^3 sec^{-1}) and O_2($k = 2.0 \times 10^{-11}$ cm^3 sec^{-1}).[42] The total reaction rate with N_2 and O_2 at 100 km is:

$$k_{N_2 + O_2} = k_{N_2}[N_2] + k_{O_2}[O_2]$$

$$= 1.2 \times 10^{-12} \times 1 \times 10^{13} + 2.0 \times 10^{-11} \times 2 \times 10^{12}$$

$$= 52 \text{ sec}^{-1}$$

Thus, the decay rate of any CO(v) produced by $O^+ + CO_2$ would decay on a 20 msec time scale. The O^+ plus O_2, N_2 reaction rates can be compared with the rate for CO_2 where, from Figure 2-2 we take $[CO_2]$ at 100 km as 2×10^9 cm^{-3}:

$$R_{CO_2} = k_{CO_2}[CO_2] = 1.2 \times 10^{-9} \times 2 \times 10^9 = 2.4 \text{ sec}^{-1}$$

representing ~4.6×10^{-2} of the O_2+N_2 rate.

If we assume that all 1.5 eV of the $O^+ + CO_2$ reaction exothermicity winds up in CO(v), (something which is quite unlikely) then an upper bound for the fraction of the ion pair creation energy can be calculated from the ratio of O^+ to total ion production (0.05), the fraction of O^+ reacting with CO_2 (0.038) and the fraction of the ion pair production energy represented by the

exothermicity of the reaction (1.5/35 = 0.043). The resulting product (0.05 x 0.046 x 0.043) is 1×10^{-4} which is significant when compared with the 4.5×10^{-5} calculated for direct electron impact.

However, our analysis of the EXCEDE Spectral data makes it unlikely that this mechanism produces the observed CO radiation - for the same reason we rejected dissociative electron impact on CO_2. As noted in subsection 2.2.1 if this mechanism dominated CO(v) production, the observed radiation would follow the CO_2 atmospheric profile rather than that for CO. Since the observed radiation matches the CO profile quite well, as demonstrated in Figure 2-4, we can rule out $O^+ + CO_2$ as the major source of CO(v). Again the major reason for the failure of this mechanism is expected to be that CO is produced with little or no vibrational excitation in this fast and presumably direct reaction.

This page intentionally left blank.

3. PRODUCTION MECHANISMS FOR VIBRATIONALLY EXCITED OZONE

3.1 Review of Ozone Properties

Ozone is a weakly bound species with an O_2-O bond energy of ~1.0 eV. It is formed throughout the upper atmosphere by the three body reaction:

$$O + O_2 + M \rightarrow O_3 + M$$

with a termolecular rate constant of $6.0 \times 10^{-34} (T/300)^{-2.3}$ cm^6 sec^{-1} for N_2 and O_2 as dominant third bodies.[43]

In the upper mesosphere and lower thermosphere O_3 is rapidly photolyzed during daylight. At night the formation reaction is balanced by reaction with atomic oxygen and atomic hydrogen

$$O + O_3 \rightarrow 2\ O_2$$

$$H + O_3 \rightarrow OH + O_2$$

with rate constants of $8.0 \times 10^{-12} \exp^{-2060/T}$ cm^3 sec^{-1} and $1.4 \times 10^{-10} \exp^{-470/T}$ respectively,[43] leading to typical O_3 profiles as plotted in Figure 2-2. A major assessment of the aeronomy of O_3 in the undisturbed mesosphere and lower thermosphere has recently been published.[44]

As illustrated in Figure 2-2, normal atmospheric O_3 profiles fall off rapidly above 95 km, leaving little ambient O_3 for vibrational excitation by electron impact or by V→V or E→V exchange processes above 100 km.

$O_3(v)$ is of interest to the EXCEDE program because of its strong ν_3 vibrational mode centered in the long-wavelength infrared region at 1042 cm^{-1} (9.6μm). The ν_3 mode has a band strength measured to be in the range of

324-355[45,46] cm^{-2} atm^{-1} at STP. Selecting the recent band strength measurement of 355 cm^{-2} atm^{-1} [45] and utilizing Penner's expression[30] as illustrated for CO in subsection 2.2 leads to a radiative lifetime of 92.7 ms.

O_3 also has two other infrared active vibrational bands, ν_1 centered at 1103 cm^{-1} (9.1 μm) and ν_2 at 701 cm^{-1} (14.1 μm). However, both of these bands are much weaker than ν_3 with reported band strengths of 9.65 and 17.9 cm^{-2} atm^{-1} at STP respectively.[44] These band strengths and frequencies correspond to radiative lifetimes of 3042 and 4059 ms. for ν_1 and ν_2 respectively.

3.2 Excitation of Ambient O_3

At night below 100 km sufficient ambient O_3 may be present to warrant consideration of mechanisms which would enhance its vibrational population.

Possible ambient excitation mechanisms include direct excitation by electron impact, E→V exchange with the metastable electronically excited species listed in Table 2-2 ($N_2(A)$, $O_2(a,b,A,A',c)$, $O(^1D, ^1S)$ and V→V exchange with $N_2(v)$ or $O_2(v)$.

3.2.1 Electron Impact Excitation of Ozone

Direct electron impact excitation is difficult to assess. complicating factor is that O_3 is subject to dissociative attachment:[46]

$$O_3 + e \rightarrow O^- + O_2 + 0.43 \text{ eV}$$

and

$$O_3 + e \rightarrow O_2^- + O - 0.6 \text{ eV} .$$

These are relatively efficient processes for thermal electrons with a rate constant of $8.9 \times 10^{-12} (T/300)^{3/2}$ cm^3 sec^{-1} where T is the electron temperature.[47] The dissociative attachment cross section is known to peak

between 1.0 and 1.5 eV for both the lowest energy (O^-) and secondary (O_2^-) processes with absolute cross sections estimated to be 10^{-18} to 10^{-17} cm^2 for each channel.[48] While the electron temperature is not well defined under EXCEDE conditions, during the beam irradiation a thermal electron effective temperature of many thousand °K is probable, leading to a dissociative attachment rate constant as large as $10^{-9} cm^3\ sec^{-1}$. With an average electron density, n_e, of order 10^6 cm^{-3} for EXCEDE beam on conditions at 100 km, ambient O_3 will not be destroyed during the beam duration since the rate for O_3 destruction can be estimated as:

$$R_{O_3} = k\,[e] = 10^{-9} \times 10^{6} = 10^{-3}\ sec^{-1}$$

However, since quantitative inelastic excitation cross sections for O_3 are not available the ratio of effective vibrational excitation to dissociative attachment cross sections is not known. Electron energy loss spectra for O_3 do show considerable structure in the 1.2 to 2.5 eV range which is predominantly associated with known O_3 excited electronic states;[49-51] while electron transmission intensity derivative measurements have indicated clear vibrational structure for an O_3^- transition in the 0.9 to 1.8 eV range.[51] Unfortunately none of these experiments give any measure of absolute vibrational excitation cross sections for inelastic electron scattering.

In summary there is some possibility that below 100 km, where night time ambient O_3 may exceed 10^8 cm^{-3}, sufficient $O_3(v)$ may be excited by direct electron impact and survive dissociative excitation to be observable. However, in the absence of quantitative e/O_3 inelastic excitation cross section measurements it is difficult to predict the amount of $O_3(v)$ which might be produced.

3.2.2 E-V Excitation of Ozone

Ambient O_3 vibrational excitation can also occur, in principle, with each of the metastable electronic species listed in Table 2-2. However, the

weakness of the O_2-O bond in O_3(~1 eV) compared to the excitation energy of these species leads to the prediction that their quenching by O_3 will generally result in O_3 dissociation:

$$O_3 + M^* \rightarrow O_2 + O + M$$

rather than production of $O_3(v)$. The energy mismatch between the metastable excitation energies of $N_2(A)$, $O(^1S)$, $O(^1D)$, O_2(A,A' and c) and CO(a) are all clearly too large to expect $O_3(v)$ production. Only $O_2(b)$ with a total electronic energy of 1.64 eV (only 0.66 eV above $O_2(a)$) and $O_2(a)$ at 0.98 eV may be capable of vibrationally exciting O_3 without dissociating it at the same time.

Laboratory investigations of O_3 quenching of $O_2(b)$ and $O_2(a)$ give some indication of the likelihood that these processes lead to $O_3(v)$. Several measurements of the $O_2(b)$ quenching rate constant by O_3 give values near 2×10^{-11} cm^3 sec^{-1} [52-54] with an O_3 dissociation fraction in the range of 0.6 to 0.7.[53,54] Thus, O_3 does effectively deactivate $O_2(b)$ and about one third of the O_3 survives the collision.

The degree of O_3 vibrational excitation in the O_3 which survives $O_2(b)$ quenching collisions is unknown. However, an upper limit, in terms of the ion pair creation energy can be estimated by noting that: 1) no more than 0.6 of the $O_2(b)$ excitation energy can be transferred to O_3 without dissociating the receiving ozone, 2) that approximately one third of the $O_3/O_2(b)$ collisions do not dissociate the O_3, 3) our estimate from subsection 2.2.4 that a limit to the fraction of the ion pair creation energy flowing through $O_2(b)$ is ~0.01 and again from subsection 2.2.4, that the $O_2(b)$ dominant quenching process, radiative decay, has a rate of 8.3×10^{-2} sec^{-1} while quenching by N_2 at 100 km proceeds at a rate of 2.2×10^{-2} sec^{-1}. From Figure 2-2 we estimate a 100 km O_3 abundance of 10^8 cm^{-3}, thus the O_3 quenching rate for $O_2(b)$ at 100 km is:

$$Q = k[O_3] = 2 \times 10^{-11} \times 10^8 = 2 \times 10^{-3} \text{ sec}^{-1}$$

or 2% of the combined radiative and N_2 quenching decay rates at 100 km.

Thus, an upper limit for the fraction of the ion pair creation energy which can flow into $O_3(v)$ at 100 km can be estimated as the $O_2(b)$ energy fraction, times the percentage of $O_2(b)$ quenched by O_3, times the fraction of quenching collisions in which O_3 survives, times the fraction of the $O_2(b)$ excitation energy which can be deposited into $O_3(v)$ without O_3 dissociation; or $0.01 \times 0.02 \times 0.67 \times 0.6 = 8 \times 10^{-5}$. This is a significant upper limit for $O_3(v)$ production from $O_2(b)$ and may well be observable. It will decay with a time scale characteristic of $O_2(b)$ radiative decay rate plus collisional quenching by N_2. As noted above at 100 km this rate is $(8.3 + 2.2) \times 10^{-2} = 0.1\ s^{-1}$ giving it a characteristic time scale of 10 s at 100 km.

On the other hand, the quenching rate for $O_2(a)$ by O_3 is very slow, as it is for most other gases. At 300°K a quenching rate constant of 3×10^{-15} cm^3 sec^{-1} has been measured[55-57] but temperature dependent experiments[56-57] indicate that the appropriate rate to use for the 200°K temperature typically found at 100 km is 4×10^{-17} cm^3 sec^{-1}, leading to a $O_2(a)$ quenching rate by O_3 at 200 km of

$$Q_{O_3} = k_{O_3} [O_3] = 4 \times 10^{-17} \times 10^8 = 4 \times 10^{-9}\ sec^{-1}$$

This compares with the O_2 quenching rate which is 10^3 times faster:

$$Q_{O_2} = k_{O_2} [O_2] = 2 \times 10^{-18} \times 2 \times 10^{12} = 4 \times 10^{-6}\ sec^{-1}$$

Furthermore, it is suspected that most of the measured $O_2(a)$ quenching reactions with O_3 lead to dissociation of O_3.[55-57]

In any event, since we concluded in subsection 2.2.4 that no more than a few percent of the ion pair creation energy can pass through $O_2(a)$ and since only about 10^{-3} of the $O_2(a)$ is quenched by O_3 we can conclude that the upper limit for $O_3(v)$ creation in the quenching of $O_2(a)$ is few times 10^{-5} of the

ion pair creation energy. When the fact that O_3 dissociation is believed to be the major product channel for $O_2(a)$ quenching is added to the very slow transfer rate it is clear $O_2(a)$ cannot produce observable $O_3(v)$ under EXCEDE conditions.

3.2.3 V→V Excitation of $O_3(v)$

As explored in subsection 2.2.3, a considerable fraction, $\sim 2.4 \times 10^{-4}$, of the ion pair creation energy is deposited in $N_2(v)$ under EXCEDE conditions. However, since rate constants for even near resonant V-V transfer processes are small, this energy must be channeled into infrared active trace species vibrational modes like CO(v) and $O_3(v)$ over very long time scales. A smaller fraction of the ion pair creation energy ($<10^{-4}$) can be expected to be deposited in $O_2(v)$.

Ozone is an unpleasant laboratory chemical, and very few laboratory vibrational quenching experiments have been reported for O_3 as a reactant. We are not aware of any V→V transfer measurements for either $N_2(v)$ or $O_2(v)$ by O_3. However, based on similar nonresonant systems such as $O_2(v)$ transferring to $CO_2(v)$ we doubt that V→V quenching rate constants for $N_2(v)$ and $O_2(v)$ by O_3 in the 200-300°K temperature range exceed 10^{-14} cm^3 sec^{-1}. Assuming this 10^{-14} upper limit we can calculate the fastest time scales for V→V transfer from $O_2(v)$ and $N_2(v)$ to O_3 as $\approx k_{V\rightarrow V} \times [O_3]$ or 10^{-14} cm^3 sec^{-1} x 10^8 cm^{-3} $\approx$ 10^{-6} sec^{-1} at 100 km. Thus, the transfer rate from $N_2(v)$ or $O_2(v)$ to O_3 has a probable time scale no shorter than 10^6 seconds or 11.6 days. Thus, no observable enhancement of $O_3(v)$ can be expected from V→V transfer under EXCEDE experimental conditions.

3.3 Chemical Production of $O_3(v)$

Above 100 km ambient O_3 drops to negligible levels and observable levels of $O_3(v)$ must be formed in a chemical reaction.

The most common atmospheric source of $O_3(v)$ is chemiluminescent production in the recombination formation reaction:

$$O + O_2 + M \rightarrow O_3(v) + M$$

Numerous laboratory experiments have demonstrated that this reaction is an efficient source of $O_3(v)$.[58-60]

However, we do not expect this reaction to contribute to the $O_3(v)$ spectrum under EXCEDE conditions because there is negligible enhancement of either O or O_2 caused by the electron irradiation process, and because the rate of O recombination with O_2 has an extremely long time scale, calculable from the O recombination rate at 100 km as:

$$R_{O + O_2 + M} = k_{O + O_2 + M} [O_2] [M]$$

$$= 6.0 \times 10^{-34} \left(\frac{200}{300}\right)^{-2.3} \text{ cm}^6 \text{ sec}^{-1} \times 2 \times 10^{12} \text{ cm}^3 \times 1.2 \times 10^{13} \text{ cm}^3$$

$$= 3.7 \times 10^{-8} \text{ sec}^{-1}$$

Thus, the time scale for O atom recombination is over 10^7 sec. at 100 km.

Clearly if an infrared chemiluminescent source of $O_3(v)$ is to be operative on EXCEDE experimental time scales it must involve a two body process. Any three body processes, involving either ground state or excited O and O_2 will have a time scale for too long to be observable under EXCEDE conditions.

We have identified one possible bimolecular source of $O_3(v)$, the reaction of O_2 with the O_2^* 4.5-5 eV states:

$$O_2^*(A, A' \text{ or } c) + O_2 \rightarrow O_3(v) + O$$

As noted in the introduction, laboratory experiments reported by Kenner and Ogryzlo in Reference 6 strongly indicate that at least one of the O_2 4.5-5 eV states can react with O_2 to produce $O_3(v)$.

Also, as reported by us in References 4 and 5, analysis of PRECEDE data indicates that as much as 6% of the beam deposition energy may result in O_2^* production. Furthermore, as discussed in subsection 2.2.4 both intrinsic radiative quenching and physical quenching of these states by atmospheric species is slow enough to allow them ample opportunity to react with ambient ground state O_2.

At the present time we have little quantitative rate information for this proposed source of $O_3(v)$, however the work reported in Reference 6 indicates a $O_2^* + O_2$ rate constant between 10^{-12} and 10^{-14} cm^3 sec^{-1}. Adopting a relatively small value of 3×10^{-14} cm^3 sec^{-1} gives an $O_3(v)$ production rate at 100 km of:

$$R_{O_2^*} = k_{O_2^* + O_2} [O_2] = 3 \times 10^{-14} \text{ cm}^3 \text{ sec}^{-1} \times 2 \times 10^{12} \text{ cm}^{-3} = 0.06 \text{ sec}^{-1}$$

Thus, $O_3(v)$ production rate is slower than the $O_2(A)$ radiative quenching rate by about a factor of 80 but comparable with the $O_2(A')$ or $O_2(c)$ radiative or collisional quenching rate. This rate estimate would give ~ 17 second time scale for the release of the copious O_2^* energy into $O_3(v)$ which may well be observable by properly designed EXCEDE experiments. The choice of the 3×10^{-14} cm^3 sec^{-1} reaction rate constant for O_2^* with O_2 is consistent with the measured quenching rate for $O_2(c)$ by O_2[39] and with our analysis identifying O_2^* as the PRECEDE long lived visible radiator.[4,5] However, it should be remembered that the $O_2^* + O_2$ rate constant is very uncertain and the actual time scale may be a factor of 10 or 100 faster. Up to 20% (~1 eV) of the O_2^* energy can be transfered into $O_3(v)$, so that as much as $0.2 \times 0.06 = 1.2 \times 10^{-2}$ of the beam deposition energy could appear in $O_3(v)$ at 100 km.

It should also be noted that current photochemical theory badly underpredicts O_3 densities above 100 km[44] and an additional O_3 production mechanism such as $O_2^* + O_2$ which is not included in current theory seems to be necessary to cure this deficiency.

4. CONCLUSIONS

4.1 CO(v) Production Yields and Time Scales

The initial production of CO(v) is dominated by direct electron impact on CO. At 100 km this source represents about 4.5×10^{-5} of the ion pair production energy and after beam termination decays with a time constant characteristic of the CO radiative decay (28.3 msec for v = 1). This source may be noticeably enhanced by additional prompt CO(v) created by $O(^1D)$ quenching.

On the time scale of tenths of seconds to tens of seconds after beam termination it is possible that E→V transfer from $N_2(A)$ and/or two of the O_2 4.5 - 5 eV states (A', c) may contribute to the CO(v) signal, however definitive predictions for these processes require better knowledge of CO(v) specific quenching cross sections for $N_2(A)$ and $O_2(A', c)$ by CO and for CO(a) by N_2, O_2, and O.

Finally, on the time scale of minutes to tens of minutes, a long-lived, low-level and slowly decaying (~10 minute) source of CO(v) will be produced from V→V exchange with $N_2(v)$.

4.2 O_3 Excitation Mechanisms

Below 100 km, excitation of ambient O_3 either by direct electron impact or by $O_2(b\ ^1\Sigma)$ quenching may lead to observable $O_3(\nu_3)$ emission on EXCEDE experimental time scales. These sources will be produced promptly and decay with the $O_3(v)$ radiative ν_3 lifetime of 92.7 msec.

A more important source of $O_3(v)$ operative at all altitudes of interest is the reaction of electron-excited O_2^* 4.5 - 5 eV states with ambient O_2. This source of $O_3(v)$ may involve as much as one percent of the ion pair creation energy, it will most likely be created with a time constant of between 5 and 50 seconds and decay on a similar time scale.

This page intentionally left blank.

REFERENCES

1. Private Communication, R. O'Neil, Air Force Geophysics Laboratory, 1981.

2. "Proceedings of the DNA Infrared Data Review Meeting", Vol. I, Defense Nuclear Agency (September, 1983).

3. M.S. Zahniser, R.B. Lyons, C.E. Kolb, F. Bien, S. Adler-Goldan, R. O'Neil, J. Winnick, E. Lee and J. Gibson, "The 4.7 Micrometer Feature in EXCEDE:SPECTRAL: A Case for Carbon Monoxide as the Emitting Species", Paper 13, Reference 2.

4. R.B. Lyons, M.S. Zahniser and C.E. Kolb, "PRECEDE Long-lived Radiator", Paper 17, Reference 2.

5. R.B. Lyons, M.S. Zahniser and C.E. Kolb, "Electron Beam Induced Long-Lived Luminescent Trail in the PRECEDE Experiment - An Analysis of Possible Sources in the Uncontaminated Atmosphere", Report No. ARI-RR-327, Aerodyne Research, Inc., Billerica, MA (April 1983).

6. R.D. Kenner and E.A. Ogryzlo, "Orange Chemiluminescence from NO_2", J. Chem. Phys. 80, 1-6 (1984).

7. M. Allen, Y.L. Yung and J.W. Waters, "Vertical Transport and Photochemistry in the Terrestrial Mesosphere and Lower Thermosphere (50-120 km)", J. Geophys. Res. 86, 3617-3627 (1981).

8. H. Ehrhardt, L. Langhans, F. Linder and H.S. Taylor, "Resonance Scattering of Slow Electrons from H_2 and CO Angular Distributions", Phys. Rev. 173, 222 (1968).

9. R.T. Clancy, D.O. Mahlemen, and G.L. Berge, "Microwave Spectra of Terrestrial Mesospheric CO", J. Geophys. Res. 87, 5009-5014 (1982).

10. K.F. Kunzi and E.R. Carlson, "Atmospheric CO Volume Mixing Profiles Determined from Ground Based Measurements of the $J = 1 \rightarrow 0$ and $J = 2 \rightarrow 1$ Emission Lines", J. Geophys. Res. 87, 7235-7241 (1982).

11. D. Offermann, V. Freidrich, P. Ross and U. VonZahn, "Neutral Gas Composition Measurements Between 80 and 120 km", Planet. Space Sci. 29, 747-764 (1981).

12. T.J. Keneshea, S.P. Zimmerman, and C.R. Philbrick, "A Dynamic Model of the Mesosphere and Lower Thermosphere", Plant. Space Sci. 26, 335 (1978).

13. P.H.G. Dickinson, W.C. Bain, L. Thomas, E.R. Williams, D.B. Jenkins and N.D. Twiddy, "The Determination of the Atomic Oxygen Concentration and Associated Parameters in the Lower Ionosphere", Proc. R. Soc., London A 369, 379 (1980).

14. R.J. Thomas and R.A. Young, "Measurement of Atomic Oxygen and Related Airglows in the Lower Thermosphere", J. Geophys. Res. 86, 7389 (1981).

15. D. Offermann, V. Friedrich, P. Ross and U. Von Zahn, "Neutral Gas Composition Measurements Between 80 and 120 km", Planet. Space Sci. 29, 747 (1981).

16. U.S. Standard Atmosphere, 1976, National Oceanic and Atmospheric Administration, NOAA-S/T 76-1562, Washington, DC (1976).

17. G. Vaughan, "Diurnal Variation of Mesospheric Ozone", Nature, 296, 133 (1982).

18. E. Hyman, J.D. Strickland, P.S. Julienne and D.F. Strobel, "Auroral NO Concentrations?", J. Geophys. Res. 81, 4765 (1976).

19. G.J. Schulz, "Resonances in Electron Impact on Diatomic Molecules", Rev. Mod. Phys. 45, 423-486 (1973).

20. L.J. Keiffer, "A Compilation of Electron Collision Cross Section Data for Modeling Gas Discharge Lasers", Report No. 13, JILA Information Center, University of Colorado, Boulder, CO (September 1973).

21. D.J. Bender, "Measurement of Vibrational Population Distributions in a Supersonic Expansion of Carbon Monoxide", Report No. 622, Institute for Plasma Research, Stanford University, Stanford, CA (March 1975).

22. A. Steed, "Preliminary Data Observation - Field Widened Interferometer Experiment", Paper 10 of Reference 2.

23. R.R. O'Neil, E.T.P. Lee and E.R. Huppi, "Auroral O(^{1}S) Production and Loss Processes: Ground Based Measurements of the Artificial Auroral Experiment PRECEDE", J. Geophys. Res. 84, 823-833 (1979).

24. M.R. Torr and D.G. Torr, "The Role of Metastable Species in the Thermosphere", Rev. Geophys. and Space Phys. 20, 91-144 (1982).

25. R.T. Bailey and F.R. Cruickshenk, "Spectroscopic Studies of Vibrational Energy Transfer", Adv. in IR and Raman Spec., 8, 52-150 (1981).

26. K. Kim, "The Integrated Intensity of the Carbon Monoxide Fundamental Band", J.Q.S.R.T. 30, 413-416 (1983).

27. C. Chucherian, Jr., G. Guelachuili and R.H. Tipping, "CO 1-0 Band Isotopic Lines as Intensity Standards", J.Q.S.R.T. 30, 107-12 (1983).

28. P.L. Varghese and R.K. Hanson, "Tunable Infrared Diode Laser Measurements of Line Strengths and Collision Widths of $^{12}C^{16}O$ at Room Temperature", J.Q.S.R.T. 24, 479-489 (1980).

29. P. Varanasi and S. Sarangi, "Measurements of Intensities and Nitrogen Broadened Linewidths in the CO Fundamental at Low Temperature", J.Q.S.R.T. 15, 475-481 (1975).

30. S.S. Penner, Quantitative Molecular Spectroscopy and Gas Emissivities, Addison-Wesley Publishing Co., Inc., Reading, MA (1959).

31. P.F. Lewis and D.W. Trainor, "Survey of Vibrational Relaxation Data for O_2, N_2, NO, H_2, HF, HCl, CO_2 and H_2O", Report No. AMP 422, Avco Everett Research Laboratories, Everett, MA (November, 1974).

32. L.G. Piper, G.E. Caledonia and J.P. Kennealy, "Rate Constants for Deactivation of $N_2(A\ ^3\Sigma_u^+, V = 0,1)$ by O", J. Chem. Phys. 75, 2847-2852 (1981).

33. L.G. Piper, G.E. Caledonia and J.P. Kennealy, "Rate Constants for Deactivation of $N_2(A)$ v = 0,1 by O_2", J. Chem. Phys. 74, 2888-2895 (1981).

34. W.G. Clark and D.W. Setser, "Energy Transfer Reactions of $N_2(A\ ^3\Sigma_u^+)$,S Quenching by Hydrogen Halides, Methyl Halides and Other Molecules", J. Chem. Phys. 84, 2225-2233 (1980).

35. L.G. Piper, "The Excitation of $O(^1S)$ in the Reaction Between $N_2(A\ ^3\Sigma_u^+)$ and $O(^3P)$", J. Chem. Phys. 77, 2373 (1982).

36. S.V. Filseth, F. Stuhl and K.H. Welge, "Collisional Deactivation of $O(^1S)$", J. Chem. Phys. 52, 239-243 (1970).

37. R.G. Shortridge and M.C. Lin, "The Dynamics of the $O(^1D_2)$ + CO (x $^1\Sigma^+$, V = 0) Reaction", J. Chem. Phys. 64, 4076-4085 (1984).

38. R.D. Kenner and E.A. Ogryzlo, "Rate Constant for the Deactivation of $O_2(A\ ^3\Sigma_u^+)$ by N_2", Chem. Phys. Lett. 103, 209-211 (1983).

39. R.D. Kenner and E.A. Ogryzlo, "Quenching of O_2 ($c^1\Sigma_u^-$) V = 0 by $O(^3P)$, $O_2(a\ ^1\Delta g)$ and Other Gases", Can. J. Chem. 61, 921-926 (1983).

40. J.A. Davidson and E.A. Ogryzlo, "The Quenching of Singlet Molecular Oxygen", in Chemiluminescence and Bioluminescence, H. Cormier et al, Ed., Plenum Press, New York (1973).

41. F.C. Fehsenfeld, E.E. Ferguson and A.L. Schmeltelkopf, "Thermal-Energy Ion-Neutral Reaction Rates III. The Measured Rate Constant for the Reaction $O^+ (^4S) + CO_2 (^1\Sigma) \rightarrow O_2 + (^2\pi) + CO (^1\Sigma)$", J. Chem. Phys. 44, 3022-3024 (1966).

42. E.E. Ferguson, "Rate Constants of Thermal Energy Binary Ion Molecule Reactions of Aeronomic Interest", Atom. Nucl. Data Tables 12, 159-178 (1973).

43. W.B. DeMore et al, "Chemical Kinetics and Photochemical Data for Use in Stratospheric Modeling", JPL Publication 83-62, Jet Propulsion Laboratory, California Institute of Technology, Pasadena, CA (September 1983).

44. M. Allen, J.I. Lunire and Y.L. Yung, "The Vertical Distribution of Ozone in the Mesosphere and Lower Thermosphere", J. Geophys. Res. 89, 4841-4872 (1984).

45. L.A. Pugh and K.N. Rao, "Intensities from Infrared Spectra", Molecular Spectroscopy, Modern Research, VII, K.N. Rao, Ed., pp. 165-225 Academic Press, New York (1976).

46. F.L. Bartman, W.R. Kuhn and L.T. Loh, "9.6 μm Ozone Band (υ_3) Intensity", J. Opt. Soc. Am. 66, 860-861.

47. G.E. Caledonia, "A Survey of the Gas-Phase Negative Ion Kinetics of Inorganic Molecules, Electron Attachment Rates", Chem. Rev. 75, 333-351 (1975).

48. R.K. Curran, "Negative Ion Formation in Ozone", J. Chem. Phys. 35, 1849 (1961).

49. R.J. Celotta, S.R. Miekzarek and C.E. Kuyatt, "Electron Energy Loss Spectrum of Ozone", Chem. Phys. Lett. 24, 428-430 (1984).

50. N. Swanson and R.J. Celotta, "Observation of Excited States in Ozone Near the Dissociation Limit", Phys. Rev. Lett. 35, 783-785 (1975).

51. R.J. Celotta, N. Swanson and M. Kurepa, "Electron Scattering from Ozone", ICPEAC X, V. 2, 656-657, Paris, France (1977).

52. P.J. Ogren, T.J. Sworski, C.J. Hochanadel and J.M. Cassel, "Flash Photolysis of O_3 in O_2 and $O_2 + H_2$ Mixtures. Kinetics of $O_2 (^1\Sigma_g^+) + O_3$ and $O(^1D) + H_2$ Reactions", J. Phys. Chem. 86, 238-242 (1982).

53. S.T. Amimoto and J.R. Wiesenfeld, "$O_2(b^1\Sigma_g^+)$ Production and Deactivation Following Quenching of $O(^1D_2)$ in O_3/O_2 Mixtures", J. Chem. Phys. 72, 3899-3903 (1980).

54. T.G. Slanger and G. Black, "Interactions of $O_2(b^1\Sigma_g^+)$ with $O(^3P)$ and O_3", J. Chem. Phys. 70, 3434-3438 (1979).

55. R.P. Wayne and J.N. Pitts, Jr., "Rate Constant for the Reaction $O_2(^1\Delta g)$ + $O_3 \rightarrow 2O_2 + O$", J. Chem. Phys. 50, 3644-3645 (1969).

56. F.D. Findlay and D.R. Snelling, "Temperature Dependence of the Rate Constant for the Reaction $O_2(^1\Delta g) + O_3 \rightarrow 2O_2 + O$", J. Chem. Phys. 54, 2350-2355 (1971).

57. K.H. Becker, W. Groth and U. Schurath, "Reactions of $O_2(^1\Delta g)$ with Ozone", Chem. Phys. Lett. 14, 489-492 (1972).

58. C.W. von Rosenberg, Jr. and D.W. Trainor, "Vibrational Excitation of Ozone Formed by Recombination", J. Chem. Phys. 61, 2442-2456 (1974).

59. T. Kleindienst, J.B. Burkholder, E.J. Bair, "The Spectrum of Ozone During Formation by Recombination", Chem. Phys. Lett. 70, 117-122 (1980).

60. W.T. Rawlins, G.E. Caledonia and J.P. Kennealy, "Observation of Spectrally Resolved Infrared Chemiluminescence from Vibrationally Excited $O_3(\upsilon_3)$", J. Geophys. Res. 86, 5247-5252 (1981).

END

9-87

DTIC